ARCHIVES OF ELECTRICAL ENGINEERING VOL. 64(1), pp. 37-51 (2015)

DOI 10.1515/aee-2015-0005

Simulation and experimental results of hybrid electric machine with a novel flux control strategy

PIOTR PAPLICKI, MARCIN WARDACH, MICHAŁ BONISŁAWSKI, RYSZARD PAŁKA

West Pomeranian University of Technology, Szczecin
Department of Power Systems and Electrical Drives
ul. Sikorskiego 37, 70-313 Szczecin, Poland
e-mail: {paplicki/marwar/michal.bonislawski/rpalka}@zut.edu.pl

(Received: 05.11.2014, revised: 22.12.2014)

Abstract: The paper presents selected simulation and experimental results of a hybrid ECPMS-machine (Electric Controlled Permanent Magnet Synchronous Machine). This permanent magnets (PMs) excited machine offers an extended magnetic field control capability which makes it suitable for battery electric vehicle (BEV) drives. Rotor, stator and the additional direct current control coil of the machine are analyzed in detail. The control system and strategy, the diagram of power supply system and an equivalent circuit model of the ECPMS-machine are presented. Influence of the additional excitation on the performance parameters of the machine, such as: torque, efficiency, speed limits and back-EMF have also been discussed.

Key words: PM machines, FEM analysis, experimental results, control strategy, field control capability, efficiency maps

1. Introduction

Requirements for more compact, energy-saving and cheaper electric machines have grown during the last two decades. In this time a great progress in the development of PMs, in the area of electric machines design and power electronics has been achieved. Therefore the attention to PM machines is constantly growing. However, the complicated control systems of conventional PM machines let the researchers develop novel machine structures with easier field control technique. New, alternative PM machine topologies with field weakening or hybrid excitation have been recognized and introduced in the literature e.g. [1-3], in order to eliminate problems associated with the field weakening techniques used in conventional PM machines.

Air gap flux control of PM machines can be realized by two main ways: control techniques and suitable modification of the machine topology. Conventional PM machines have a fixed magnet excitation which limits the drive's performance in over-speed region and becomes a significant limitation. The machines are operated at constant U/f ratio up to base speed ω_b and constant voltage operation which requires weakening of the magnetic field at higher

speeds to extend the operation range. Above the base speed, vector control techniques are typically used to weaken the air gap flux and unfortunately they result in a decrease of drive system efficiency. However these techniques require a large demagnetization stator current in the *d*-axis to flow in the machine and cause increased losses and demagnetization risk of the magnets.

Nowadays, a number of alternative design solutions exist to eliminate these problems in PM machines. Additionally the possibility of controlling the air gap flux of new hybrid constructions extends the field weakening capability and provides a method to improve the efficiency of the drive system.

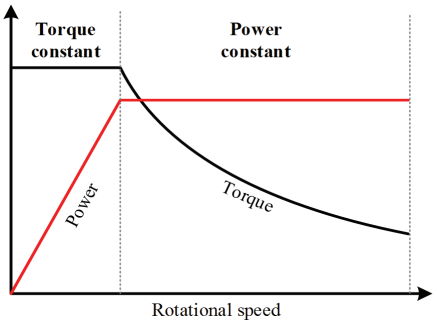

Fig. 1. BEV's traction characteristics

Development of electrical machines used in the BEV is very complex and requires special approaches [4-6]. According to operating conditions a traction characteristic, as shown in Figure 1, implies the use in two operation regions: constant torque and constant power. It should be noted that extended constant power range capability is extremely important to eliminate the use of multiple gear ratios and to reduce the power supply volt-ampere rating.

Features of hybrid machines allow increasing the flux control range due to additional electrical circuits. Hence, there is a possibility to produce high torque (e.g. during starting and acceleration of the vehicle) or extend maximal speed while reducing stator currents of the machine.

2. Types of hybrid machines

There are many design solutions of hybrid PM machines which can be used for the flux weakening. Typically these machines have two excitation sources: PMs and DC windings. Generally, hybrid machines can be classified into two groups: serial and parallel configurations [7-8]. In the serial configuration, the magnetic flux exited by additional winding passes through the PMs, and in the parallel configuration the flux is associated with the additional windings but it doesn't pass through the PM, due to its relatively high reluctance (Fig. 2).

Different classifications of hybrid machines take the location of the excitation circuits into account. The first type possesses an additional excitation winding fixed on the rotor, the se-

cond on the stator, and in case of the third type – the circuits are present on both the rotor and the stator of the machine.

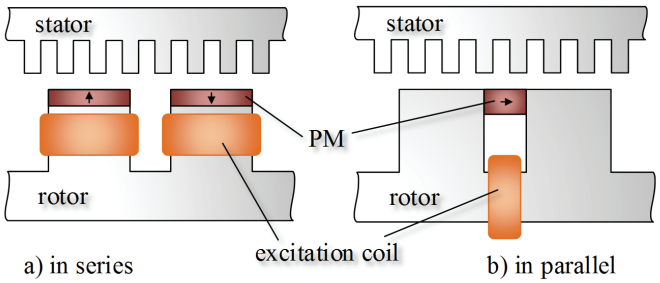

Fig. 2. Configuration of serial and parallel hybrid machines

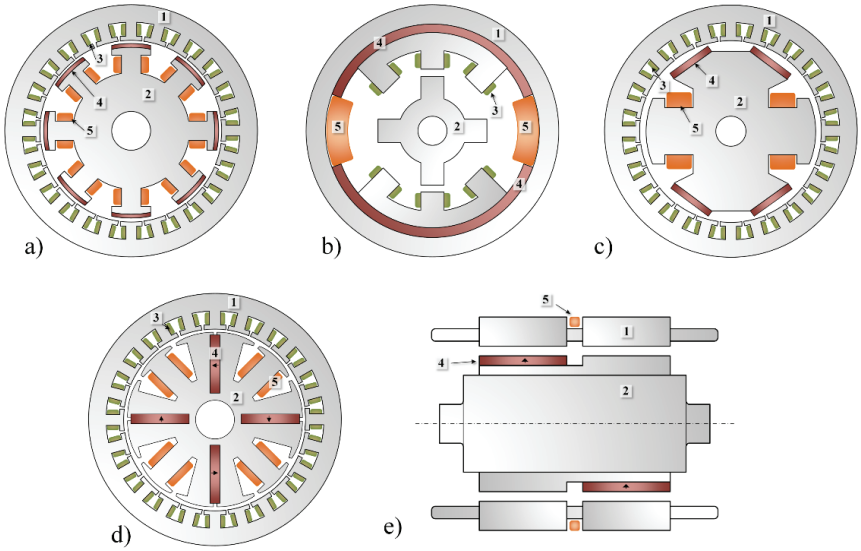

Fig. 3. Selected hybrid machine topologies: a) stator; b) rotor; c) armature winding; d) PM; e) additional excitation winding

Figure 3a shows the serial hybrid machine topology which consists of the PMs and the additional DC windings in the rotor. The disadvantage of such configuration arises from the necessity of using slip rings to supply the DC windings [9]. The construction shown in Figure 3b is also a serial structure, but two sources of magnetic field excitation are arranged in the stator.

Generally, the serial configuration allows a small range of the flux control. Additionally, the main disadvantage of most of the serial structures is a danger of PMs demagnetization [10], but the advantage is a simple design and high torque-to-weight ratio, as well.

Figures 3c and 3d show selected parallel design solutions where both excitation sources are located on the rotor. Therefore supplying the excitation windings requires slip rings [11].

Mixed locations of the circuits, where the additional excitation winding is fixed on the stator (Fig. 3e), don't have disadvantages mentioned above.

It should be noted that other methods for air gap flux control through the variable axial rotor/stator alignments are also known [8]. Unfortunately, the disadvantage in this type of machine construction is associated with the low torque-to-weight ratio and the significant complexity of the design.

3. ECPMS-machine

Figure 4 shows a 3-phase design of a prototype ECPMS-machine having the 12-pole double inner rotor with 2 sheeted stator cores. Armature windings are located in 36 slots in each of the two stator stacks. On the one side of the machine the rotor is formed by the exhibited single polarity PMs along with iron poles, made from a soft magnetic composite (SMC) material. On the other side of the machine the same arrangement is positioned with PMs of inverse polarity.

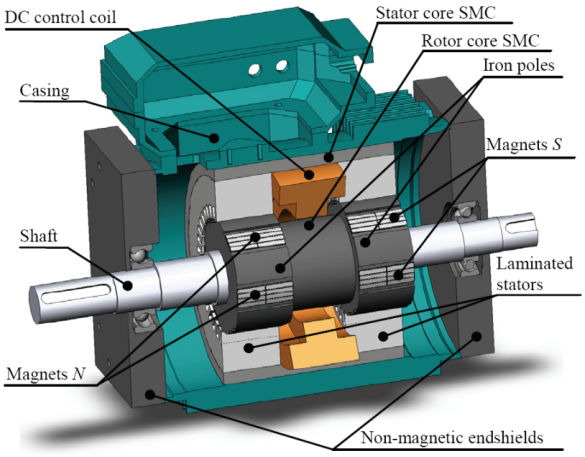

Fig. 4. Cross section of the ECPMS-machine

Presented machine topology allows applying a DC field weakening technique used in hybrid machines. In this case, in order to realize field excitation control to increase or decrease the magnetization level of the machine, an additional DC control coil is centrally mounted inside the stator SMC core, between two laminated stators. The flux generated by PMs passes through the laminated stator cores pole pieces, and it crosses the air gap of the machine in the radial direction. A main portion of the flux is passed through the stator SMC core in the axial direction, and it is returned via the rotor SMC core. The remaining part of the flux, excited by PM passing through the stator cores, returns to the iron pole SMC of the rotor. It should be noted that the flux passing through the iron pole is very important from the point of view of a field-weakening capability of the analyzed machine.

3.1. FEM analysis and simulation results

Theoretical investigation of the ECPMS-machine [12] revealed that the optimal design of the machine can be successfully performed based on a FEM (finite element method) analysis. Assuming that, in order to seek for the optimal design of the machine, the reluctance of the air gap and associated with it a geometry $\delta_{\text{IP-PM}}$ parameter should be thoroughly analyzed by FEM calculations. In this case the parameter $\delta_{\text{IP-PM}}$ means the difference $d_{\text{IP}} - d_{\text{PM}}$ and characterizes the weakening and strengthening capabilities of the machine, where d_{IP}, d_{PM} is the rotor outer diameter in front of the iron pole and the magnets, respectively. During FEM analysis (according to Fig. 5), the geometry parameter $\delta_{\text{IP-PM}}$ is fixed in the range 0 to 4.0 mm, and parameters: d_{IP} = 164 mm, d_{s1} = 165 mm (inner diameter of the stator), d_{s2} = 287 mm (outer diameter of the stator) are constant.

To accurately calculate components of a no-load magnetic flux density and to predict the electromagnetic torque of the machine an adequate 3-dimensional finite element model (3-D FEModel) was developed (Fig. 6), taking into account nonlinear B-H curves and the machine's lack of symmetry. Figure 7 shows the magnetization curves for the laminated and SMC materials.

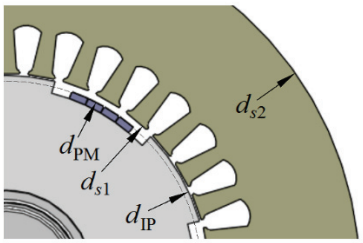

Fig. 5. Cross section of the ECPMS-machine

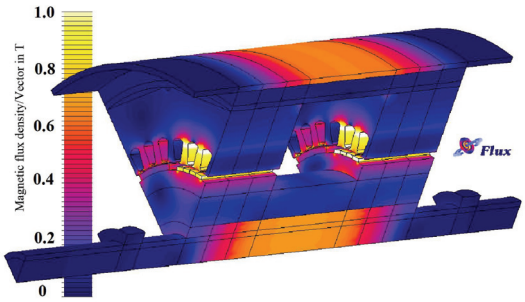

Fig. 6. Magnetic field distribution within the 3-D FEModel of the ECPMS-machine

During design and simulation investigations it was assumed that the final shape of each magnetic pole is arranged by NdFeB rectangular magnets of the N38SH-type with material and magnetic parameters as follows: 3/7/40 mm (high/width/length); B_r = 1,22 T; $H_{cB(\text{min.})}$ = 911 kA/m; ρ = 144 μΩ·cm; T_{max} = 150°C. Simulation results (Fig. 8) show that an increase of the air-gap reluctance in front of the magnets (by increasing the $\delta_{\text{IP-PM}}$ parameter) extends the range of field wakening capability. It should be pointed out that it also causes a reduction of the power density of the machine.

Moreover, all characteristics presented in Figure 8 show that the occurrence of the asymmetry in the magnetic circuit of the machine is also associated with additional excitation. A no-load distribution of magnetic field is determined by the magnets. Orientation of the magnetic field inside the shaft and the outer stator elements imposes magnets polarity. This causes that counteracting the magnetic field of the magnets at the strengthening state by DC control coil is less efficient than at its weakening. Moreover, it should be noted, that the magnetic

saturation strongly affects the leakage flux of the machine. It has been confirmed in subsequent experimental studies.

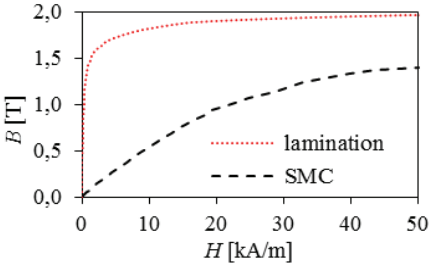

Fig. 7. Magnetization curves of the laminated material and the SMC

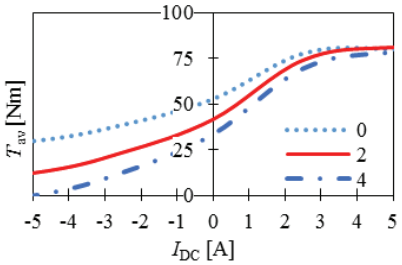

Fig. 8. Electromagnetic torque vs. DC control coil current for selected $\delta_{IP\text{-}PM}$

Additionally, the simulation results show that the DC coil current over 5A saturates the magnetic circuit and the flux control of the machine stops proper operation. Based on these results the finally accepted $\delta_{IP\text{-}PM}$ = 2 mm, which corresponds to 3 mm length of the air gap measured in front of the magnets.

3.2. Prototype construction technology

Accordingly to simulation results, a unique technology of the ECPMS-machine has been developed. Figure 9 shows a rotor of the ECPMS-machine construction which consists of two identical parts. One of them includes eight PMs with the outside magnetization direction (north pole polarization), and the second one eight PMs magnetized in the opposite direction.

As mentioned above the specific feature of the machine is the existence of an additional DC control coil located between two laminated stators (Fig. 10). This coil can be supplied by the DC-chopper via stator-fixed terminals in order to control the excitation field of the machine. Stators are located inside the bushing core made from magnetic powder material (Somaloy 500 + Kenolube 0,5%) with epoxy resin (SMC). Moreover, it should be pointed out, that the SMC material was used in the rotor core and iron pole technology.

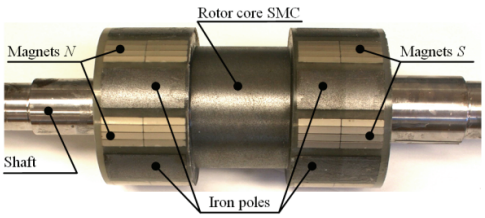

Fig. 9. Rotor of ECPMS-machine

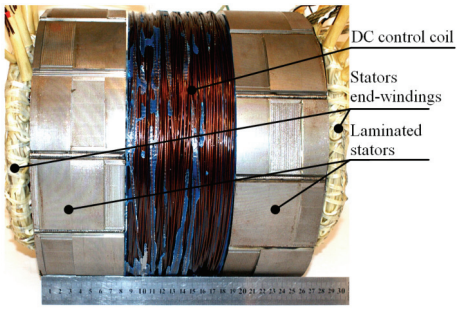

Fig. 10. Stator of ECPMS-machine

4. Equivalent circuit model of the ECPMS-machine

A control strategy (in a steady state and in transient modes) and a new approach to control the power supply system of the machine in the field weakening/strengthening range, or in a fault mode of operation, involves defining an adequate mathematical model of the machine. Following assumptions have been made:

- symmetric armature windings,
- constant resistance and inductance of windings,
- constant flux of magnets,
- higher harmonics of magnetic flux density in the air are neglected.

The basic voltage and flux equations of the machine [13-14] can be expressed as:

$$\begin{aligned} \Psi_{\mathrm{d}} &= L_{\mathrm{d}} i_{\mathrm{d}} + \Psi_{\mathrm{PM}} + M_{\mathrm{DC}} i_{\mathrm{DC}} \\ \Psi_{\mathrm{q}} &= L_{\mathrm{q}} i_{\mathrm{q}}, \end{aligned} \tag{1}$$

$$\begin{aligned} u_{\mathrm{d}} &= R_{\mathrm{s}} i_{\mathrm{d}} + \frac{\mathrm{d}\Psi_{\mathrm{d}}}{\mathrm{d}t} - \omega_{\mathrm{e}} \Psi_{\mathrm{q}} \\ u_{\mathrm{q}} &= R_{\mathrm{s}} i_{\mathrm{q}} + \frac{\mathrm{d}\Psi_{\mathrm{q}}}{\mathrm{d}t} + \omega_{\mathrm{e}} \Psi_{\mathrm{d}}, \end{aligned} \tag{2}$$

$$u_{\mathrm{DC}} = R_{\mathrm{DC}}\, i_{\mathrm{DC}} + L_{\mathrm{DC}} \frac{\mathrm{d}i_{\mathrm{DC}}}{\mathrm{d}t} - M_{\mathrm{DC}} \frac{\mathrm{d}i_{\mathrm{d}}}{\mathrm{d}t}, \tag{3}$$

$$T_{\mathrm{e}} = \frac{3}{2} p \left(i_{\mathrm{q}} \Psi_{\mathrm{d}} - i_{\mathrm{d}} \Psi_{\mathrm{q}} \right) = \frac{3}{2} p \left[\overbrace{\Psi_{\mathrm{PM}} i_{\mathrm{q}}}^{T_{synch.}} + \overbrace{M_{\mathrm{DC}} i_{\mathrm{DC}} i_{\mathrm{q}}}^{T_{DC}} + \overbrace{(L_{\mathrm{d}} - L_{\mathrm{q}}) i_{\mathrm{d}} i_{\mathrm{q}}}^{T_{rel.}} \right], \tag{4}$$

hence:

$$\begin{aligned} u_{\mathrm{d}} &= R_{\mathrm{s}} i_{\mathrm{d}} + L_{\mathrm{d}} \frac{\mathrm{d}i_{\mathrm{d}}}{\mathrm{d}t} + M_{\mathrm{DC}} \frac{\mathrm{d}i_{\mathrm{DC}}}{\mathrm{d}t} \overbrace{- \omega_{\mathrm{e}} L_{\mathrm{q}} i_{\mathrm{q}}}^{e_{\mathrm{d}}} \\ u_{\mathrm{q}} &= R_{\mathrm{s}} i_{\mathrm{q}} + L_{\mathrm{q}} \frac{\mathrm{d}i_{\mathrm{q}}}{\mathrm{d}t} + \overbrace{\omega_{\mathrm{e}} \left(L_{\mathrm{q}} i_{\mathrm{q}} + \Psi_{\mathrm{PM}} + M_{\mathrm{DC}} i_{\mathrm{DC}} \right)}^{e_{\mathrm{q}}} \end{aligned} \tag{5}$$

where: e_{d}, e_{q} – electromechanical conversion; T_{sync} – synchronous torque proportional to the i_q *(q*-axis currents*),* Ψ_{PM} flux linkage of magnets; T_{DC} axillary control torque proportional to value and direction of current (i_{DC}); T_{rel} – reluctance torque. According to these equations, the required electromagnetic torque resulting from different values of stator current components (i_{d} and i_{q}) and the additional coil current i_{DC} can be obtained.

5. Control system structure

The test setup consists of a dedicated power converter, microprocessor controller and measurement equipment. ECPMS-machine is supplied by a three-phase voltage inverter and a DC-DC converter is used to supply the control coil (Fig. 11).

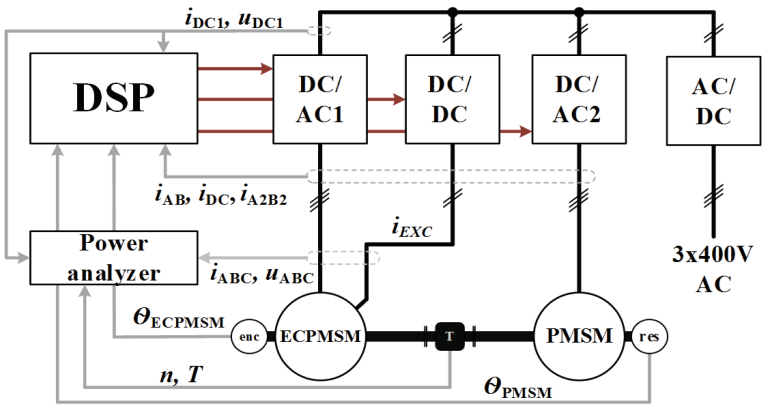

Fig. 11. Construction diagram of the test setup

Additionally, in order to perform comprehensive experimental tests and a full digital control of the ECPMS-machine, a digital signal processor (DSP) C2000 Texas Instruments TMS320F28335 was used. Moreover, a Field Oriented Control (FOC) algorithm with PI regulator, independently working on *d* and *q* axis current components has been implemented.

The system is characterized by acceptable accuracy in the current control mode. Output signals of current regulators are converted to the coordinates associated with the stator ($\alpha\beta$ and ABC), and then they are forwarded to the Space Vector Modulator (SVM) to achieve a required voltage vector.

In order to determine the mechanical characteristics, efficiency maps and dynamic phenomena, an experimental set-up shown in Figure 12 was built. The test stand was additionally equipped with the digital power analyzer (Norma 5000, Fluke), digital oscilloscope (DPO 7054, Tektronix), torque meter (Dataflex 32/100), incremental encoder and resolver to determine the shaft position. All controls and measurements are connected to the overarching PC computer with Matlab environment. PMSM 8LSA75-3000 (Bernecker & Rainer) machine was used as the load.

5.1. Preliminary experimental results

Figure 13 shows Back-EMF waveforms for three different values of the DC control coil current I_{DC} = 2; 0; –2A, at 1000 rpm velocity, and it also shows a real weakening and strengthening capability of the machine. Moreover, in Figure 14 it is shown, that 1st, 5th, 7th and 11th harmonic in no-load back-EMF waveform are present.

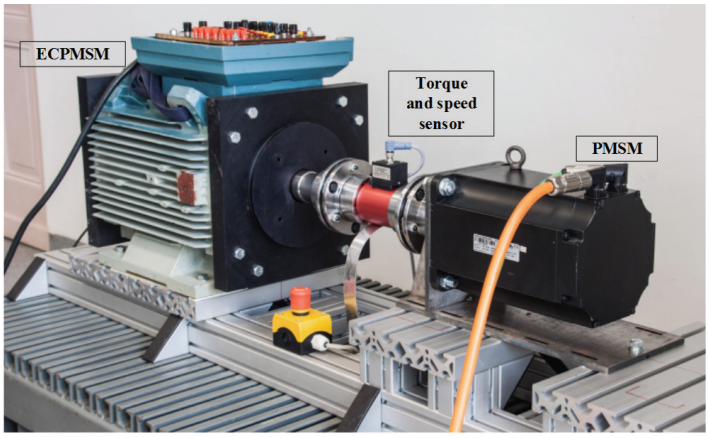

Fig. 12. Experimental set-up

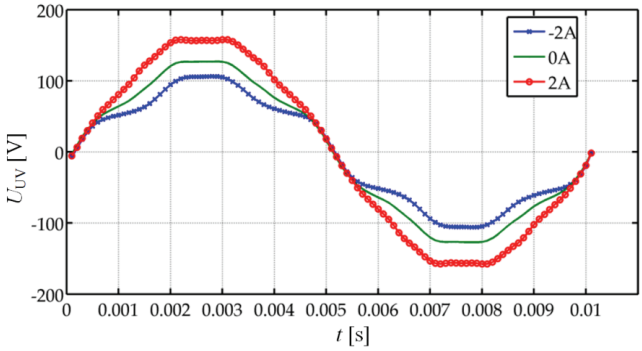

Fig. 13. Back-EMF phase-to-phase waveforms at 1000 rpm for the selected values of the DC control coil current

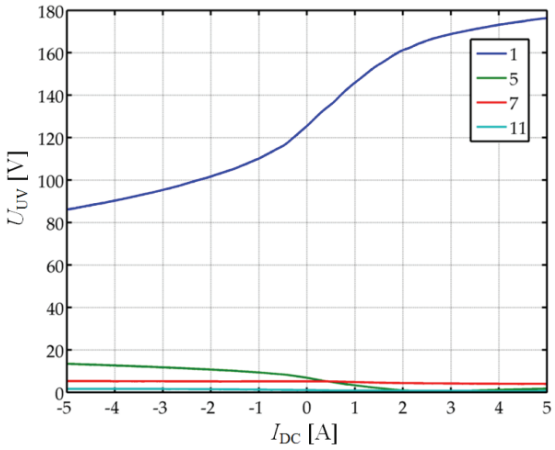

Fig. 14. Harmonic in the Back-EMF at 1000 rpm vs. DC control coil current

Using the experiment test stand efficiency maps of the machine for three cases of the DC control coil supply (I_{DC} = 2 A, 0 A and –2 A), have been measured and plotted (Fig. 15). Presented results for different operating points of the machine have been obtained under maximal torque of the load (up to 30 Nm) and the voltage in the DC bus up to 300 V.

From the overall analysis two important conclusions can be drawn: It is possible to extend the range of speed and torque of the machine using the additional coil and it is possible to increase the efficiency of the machine at the selected operating points.

5.2. Novel automatic field weakening control strategy

For the PM synchronous machine (PMSM), in the high-speed range, the voltage induced in the stator windings (proportional to the angular velocity) may be too high to suppress stator coil current control at the required level. The output voltage of the power converter can be increased, but the limitation is the maximum supply voltage of the DC bus [15-16] and the permitted voltage of stator windings of the machine resulting from the technology of the winding insulation. The consequence is the limit of the maximum speed to base speed for no-load operation (I_q = 0 A), it means:

$$\omega_b = \frac{\sqrt{U_s^2 - R_s^2 I_d^2}}{\Psi_s}. \tag{6}$$

For each PMSM it is possible to increase the speed range by reducing the stator flux:

$$\Psi_s = \frac{E_{s\max}}{\omega_{ref}}. \tag{7}$$

The adjustment of Ψ_s (at a fixed operation point) is done by I_d component of the stator current:

$$\begin{aligned} \Psi_s &= \sqrt{\Psi_d^2 + \Psi_q^2} \\ \Psi_d &= I_d L_d + \Psi_{pm} \\ \Psi_q &= I_q L_q. \end{aligned} \tag{8}$$

There exist numerous methods of field weakening operation mode control of PM machines. One of them is based on mathematical model of the machine. The stator currents (both I_d and I_q) are determined offline and then their values are saved in the control system (a "look-up table" method) [15].

Second possibility is the online method based on a difference between the required voltage $|U_s| = \sqrt{u_{sd}^2 + u_{sq}^2}$ and the maximal, achievable voltage $U_{max} = U_{DC}/\sqrt{3}$. If the value of the required voltage exceeds the possibility of the inverter, the d-axis current will be adjusted to reduce the flux (by a PI-type controller) [17].

In order to perform a preliminary analysis of the hybrid machine in the flux weakening operation the above mentioned method was modified. After reaching the base speed (resulting

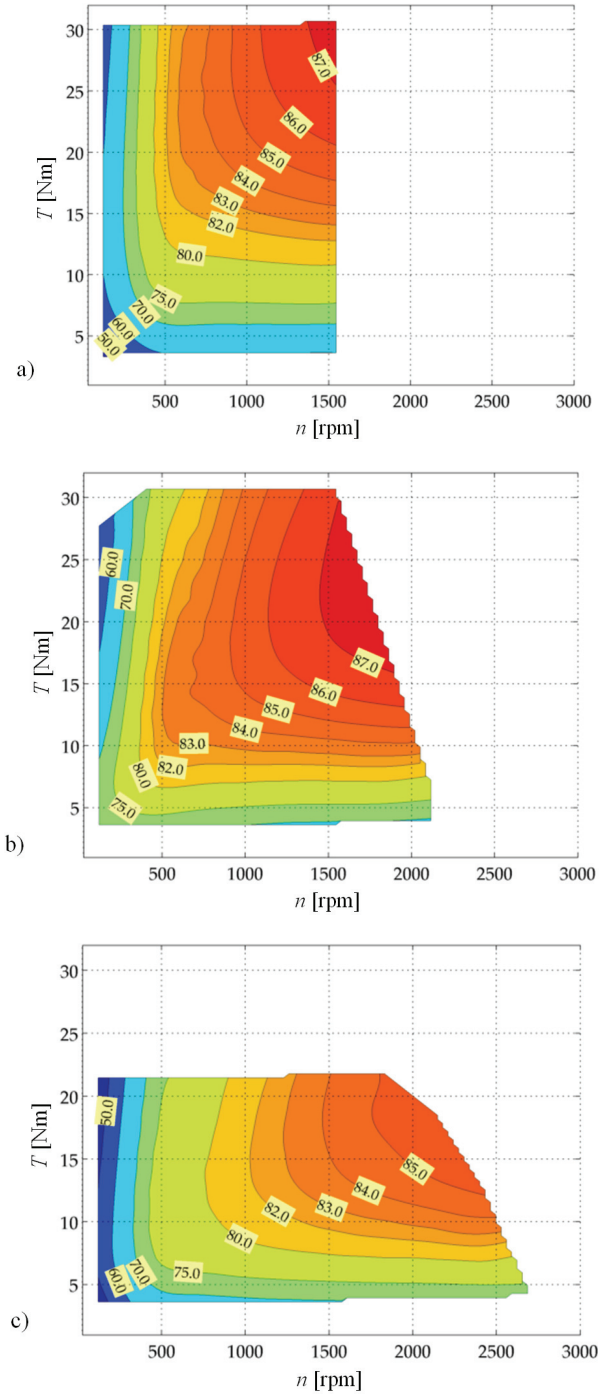

Fig. 15. Efficiency maps for a) I_{DC} = 2 A; b) I_{DC} = 0 A; c) I_{DC} = −2 A

from the limits of the inverter voltage output), the flux Ψ_s id reduced by the DC coil adjust (instead of the in *d*-axis current, Eq. (1)).

Diagram of the power and control systems, with implemented automatic flux weakening method in the hybrid ECPMS-machine, is shown in Figure 16.

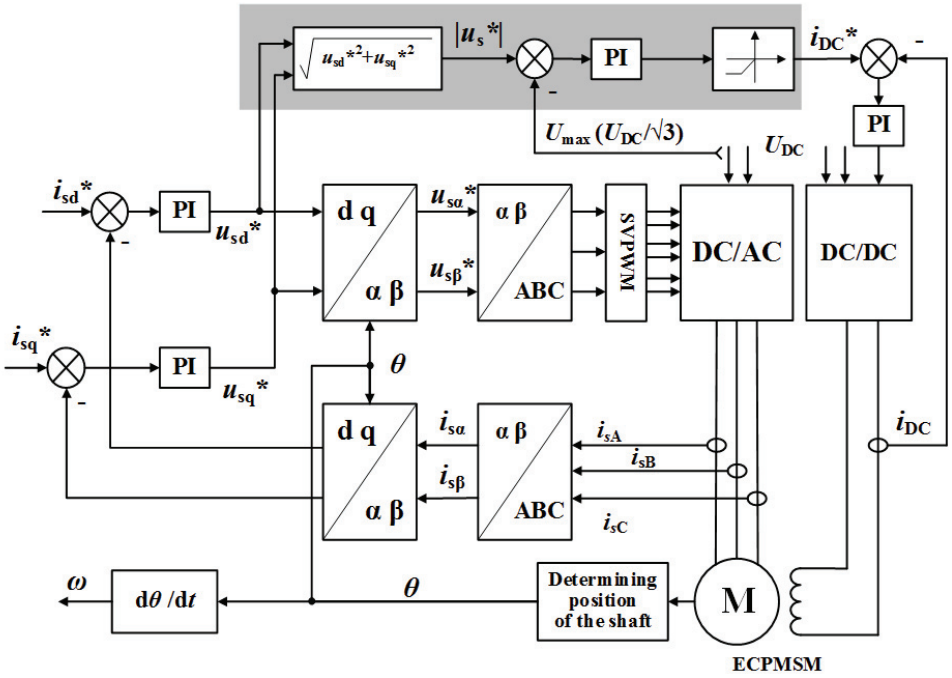

Fig. 16. Diagram of power system with implemented automatic flux weakening method for the hybrid ECPMS-machine

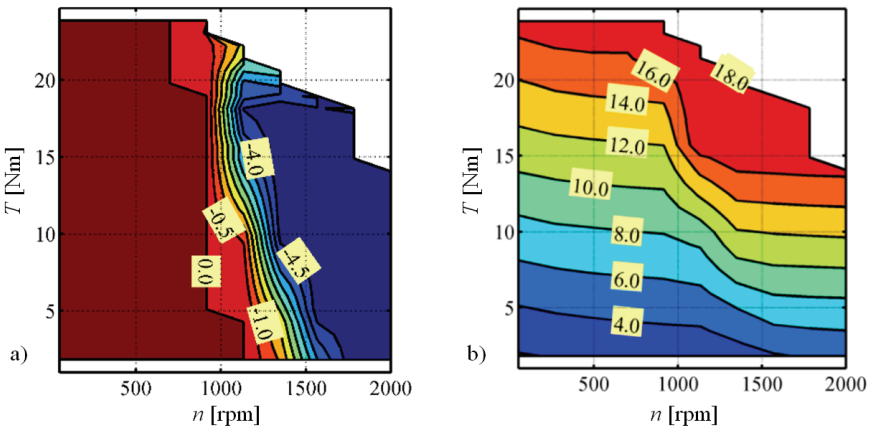

Fig. 17. Maps of winding currents in: a) DC control coil; b) armature (RMS value)

The operation principles of the automatic methods of weakening the flux using the DC control coil current, are shown in Figure 17. The base speed of the unloaded machine in this case is calculated at approx. 1100 rpm. At the base speed, the current in DC control coil was introduced, with proper direction and value, in order to obtain required machine torque, while the current component in the *q*-axis can be increased. Adjustment range of I_{DC} current has been limited between –5 A to 0 A.

The presented method of automatic flux reduction in the hybrid ECPMS-machine (only by I_{DC} current) allows to extend the speed over the base speed point. It should be noted that thermal losses generated in the DC control coil may be an important component of overall losses in the ECPMS-machine.

6. Proposal for further research

Based on machine model and experimental results the predicted performance (range of speed and torque) of the machine was estimated. In Figure 18 mechanical power maps for four cases of predicted torque and velocity changes at various control strategies have been shown. In these studies the maximum power supply voltage of 300 V and stator current up to 30 A were assumed.

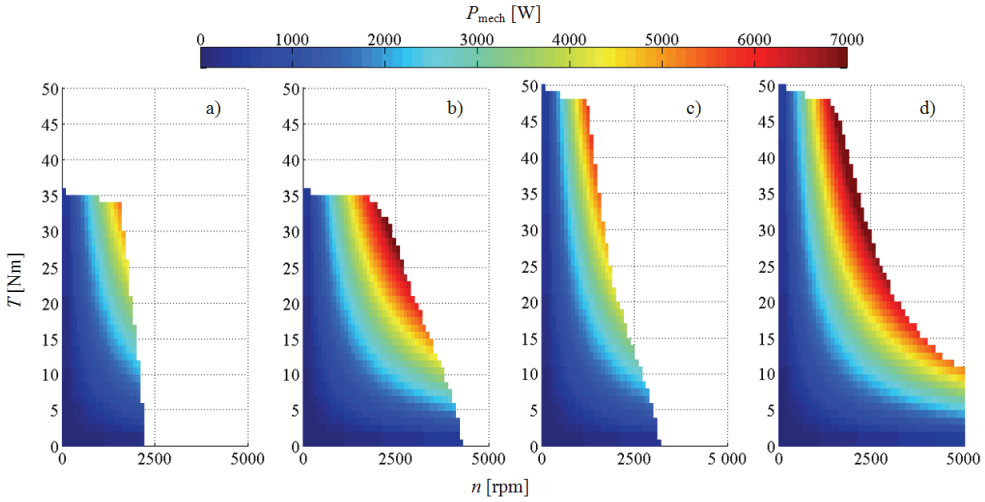

Fig. 18. ECPMSM predicted operation regions for four control strategies of currents: a) I_q; b) I_d, I_q; c) I_q, I_{DC}; d) I_d, I_q, I_{DC}

Simulation results show that the control of the stator current component in the *d*-axis (Fig. 18b) allows to increase the speed limit of the machine by a factor of approx. 2 times compared to strategy of controlling of the current in *q*-axis only (Fig. 18a). Moreover, the DC coil current control strategy (Fig. 18c) enables to increase the starting torque and the torque at the low speed range, but it doesn't allow to significantly increase the speed limits of

ECPMSM prototype. So, it can be concluded, that in order to achieve a widest range of operating points of the presented ECPMS-machine (Fig 18-d), the current control strategy must consider each component of the stator current windings I_d, I_q, I_{DC}. It will be the subject of further research.

7. Conclusions

The paper presents selected simulation and experimental results of a prototype hybrid machine with PMs and extended excitation control features. Obtained test results show noticeable influence of the DC control coil current on the field control range of the machine. The presented analysis shows the possibility to achieve required electromagnetic torque with appropriate values of the stator current (I_d, I_q) and the current in the DC control coil.

According to experimental results, it can be concluded, that a field-weakening ratio (as a ratio of a back-EMF value at field strengthening to weakening of the field) equal to 1.6:1 is effectively obtained.

Moreover, simulation results show that the proposed machine and novel control system and strategy (of all stator currents) can offer an effective flux control method allowing to extend the maximal speed over 2 times (with respect to no excitation control strategy) at constant-power range.

References

[1] Putek P., Paplicki P., Palka R., *Topology Optimization of rotor poles in a Permanent – Magnet machine using Level Set method and Continuum Design Sensitivity Analysis.* The International Journal for Computation and Mathematics in Electrical and Electronic Engineering (COMPEL) 33(3): 711-728 (2014).

[2] Putek, P., Paplicki P., Palka R., *Low cogging torque design of Permanent-Magnet machine using modified multi-level set method with total variation regularization.* IEEE Trans. Magn. 50(2), article no. 7016204 (2014).

[3] Paplicki P., *Modified concept of axial-flux permanent magnet machine with field weakening capability*. Archives of Electrical Engineering 63(2): 177-185 (2014).

[4] Liang K., Xuhui W., Shan X., Tao F., *The study of bypass hybrid excitation synchronous motors with extended field-weakening capability.* Electr. Mach. pp. 3627-3631 (2008).

[5] Chau K., Chan C., Liu C., *Overview of permanent-magnet brushless drives for electric and hybrid electric vehicles.* Ind. Electron. IEEE 55(6): 2246-2257 (2008).

[6] Wardach M., Paplicki P., Palka R., Cierzniewski P., *Influence of the rotor construction on parameters of the electrical machine with permanent magnets*. Electrical Review 11: 131-134 (2011).

[7] Nedjar B., Hlioui S., Lecrivain M. et al., *Study of a new hybrid excitation synchronous machine, in Electrical Machines (ICEM),* 2012 XXth International Conference on Electrical Machines, pp. 2927-2932 (2012).

[8] Owen R.L., Zhu Z.Q., Wang J.B. et al., *Review of Variable-flux Permanent Magnet Machines*. Journal of International Conference on Electrical Machines and Systems 1(1): 23-31 (2012).

[9] Fodorean D., Djerdir A., Viorel I.-A., Miraoui A., A *Double Excited Synchronous Machine for Direct Drive Application, Design and Prototype Tests, Energy Conversion*. IEEE Trans. 22(3): 656-665 (2007).

[10] Amara Y., Hlioui S., Belfkira R. et al., *Comparison of Open Circuit Flux Control Capability of a Series Double Excitation Machine and a Parallel Double Excitation Machine.* Veh. Technol. IEEE Trans. 60(9): 4194-4207 (2011).
[11] Luo X., Lipo T.A., *A synchronous/permanent magnet hybrid AC machine.* Energy Conversion, IEEE Trans. 15(2): 203-210 (2000).
[12] Paplicki P., *Design optimization of the electrically controlled permanent magnet excited synchronous machine to improve flux control range.* Electronika ir electrotechnika 20(10): 17-22 (2014).
[13] Zhang Z., *Maximum torque control of hybrid excitation synchronous machine drives based on field current self-optimizing method.* IECON 2013 – 39th Annual Conference of the IEEE Industrial Electronics Society, pp. 2977-2982 (2013).
[14] Mbayed R., Salloum G., Vido L. et al., *Optimal control of the hybrid excitation synchronous machine for electric propulsion in electric vehicle*. 15th European Conference on Power Electronics and Applications (EPE)): 1-10 (2013).
[15] Lin P.Y., Lai Y.S., *Novel Voltage Trajectory Control for Flux Weakening Operation of Surface Mounted PMSM Drives.* Industry Applications Society Annual Meeting, IAS '08. IEEE): 1-8 (2008).
[16] Paplicki P., Piotuch R., *Improved Control System of PM Machine with Extended Field Control Capability for EV Drive.* Mechatronics – Springer International Publishing, Ideas for Industrial Application 317. pp. 125-132, DOI: 10.1007/978-3-319-10990-9_12 (2015)
[17] Kwon T.S., Sul S.K., *A novel flux weakening algorithm for surface mounted permanent magnet synchronous machines with infinite constant power speed ratio.* Electrical Machines and Systems ICEMS, pp. 440-445 (2007).